A Novel Evolution Strategy and its Application to Inverse Scattering in Microwave Imaging

Lin Yang[1], Shiyou Yang[2], S. L. Ho [1], Weinong Fu[1] and Lei Liu[2]
[1] Department of Electrical Engineering, The Hong Kong Polytechnic University, Hong Kong
[2] College of Electrical Engineering, Zhejiang University, Hangzhou, 310027, China

Abstract —An inversion methodology for microwave imaging based on an improved evolution strategy algorithm is proposed. The nonparametric mutation process, adaptive trade-off between exploration and exploitation, small population size and non-revisiting property is well-suited for solving expensive evaluation inverse problem. The numerical results as reported confirm positively its feasibilities and advantages.

***Index Terms*—Inverse scattering, microwave imaging, Evolution Strategy, numerical method.**

I. Introduction

Different inversion procedures have been developed for microwave imaging techniques by virtue of their exclusive merits and potentials in engineering applications. The most common and robust procedure is to recast the imaging problem into a minimization one, in which the second-order Born approximation (2BA) is used for scattered electric field computations [1].

The reversion is generally solved using a stochastic optimal algorithm [1]. However, the situations with both convergent speed and reversion accuracy of available approaches are still unsatisfactory. In this regard, a methodology based on improved evolution strategy (ES) algorithm is proposed.

To reduce the heavy computational burden of available stochastic optimal algorithms while guaranteeing their global search abilities, this paper puts forward two useful methods to improve the algorithm: 1) a completely derandomized self-adaptation scheme called covariance matrix adaptation (CMA) [2] is used. It can be improved by utilizing an evolution path rather than single search steps. The adaptation of strategy parameters in proposed algorithm takes place in the concept of mutative strategy parameter control (MSC). Strategy parameters are mutated and a new search point is generated by means of this mutated strategy parameter setting. 2) Proposes one solution to the revisit problem in the context of ES. We use an archive design using binary space partitioning (BSP) tree [3]. It not only is an efficient method to check for revisits and reduce the searching space and itself constitutes a novel adaptive mutation operator that has no parameter, which could perfectly overcome the shortcomings of CMA.

Due to the inefficiency of Born-type approximations in scattered electric field computations, the frequency-domain finite element method is used to increase the accuracy of the field computations. To consider open boundaries, the second-order absorbing boundary conditions are used.

II. Models and Methods

When a scatterer is illuminated by a single frequency *TM* incident wave, there will be conduction current or polarization current on its surface and in its body as shown in Fig.1.

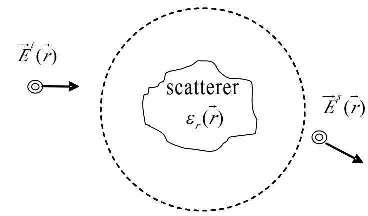

Fig. 1. Geometric configuration of two-dimensional scattering case

Considering a nonmagnetic isotropic inhomogeneous lossy cylindrical scatterer in a finite space $V \subset R^3$, when the scatterer is successively illuminated in the free space by some known magnetic waves (TM_z), there will be an electric field polarized in the z direction. Under these assumptions, the incident field $\vec{E}^i(\vec{r})$, the scattering electric field (secondary radiation) $\vec{E}^s(\vec{r})$ and the total field $\vec{E}(\vec{r})$ would satisfy the following Lippmann-Schwinger integral equation

$$\begin{aligned}\vec{E}(\vec{r}) &= \vec{E}^i(\vec{r}) + k_0^2 \int_V \vec{E}(\vec{r}')[\widetilde{\varepsilon}_r(\vec{r}') - 1] G(\vec{r}, \vec{r}') dV' \\ &+ \int_V \nabla\{\nabla \bullet \vec{E}(\vec{r}')[\widetilde{\varepsilon}_r(\vec{r}') - 1]\} G(\vec{r}, \vec{r}') dV'\end{aligned} \quad (1)$$

where, $\vec{r} \in R^3$ represents the observing point, $\vec{r}' \in V$ is the source region, $\widetilde{\varepsilon}_r(\vec{r}') = \varepsilon_r(\vec{r}') - \dfrac{j\sigma(\vec{r}')}{\omega \varepsilon_0}$, $\varepsilon = \varepsilon_r \varepsilon_0$ represents the permittivity of the surrounding background, $G(\vec{r}, \vec{r}')$ is the free space Green's function and is given by

$$G(\vec{r}, \vec{r}') = e^{-jk_0\left|\vec{r} - \vec{r}'\right|} \Big/ 4\pi \left|\vec{r} - \vec{r}'\right| \quad (2)$$

For a two-dimensional (2D) problem, if the scatterer is weak enough. As a result, the total electric field can be approximated by the second-order Born approximation. Using this approximation, one obtains the scattering field as

$$E^S(\vec{r}) \approx E^{(2)}_{Born}(\vec{r}) = \int_V [\vec{E}^i(\vec{r}') + E_{Born}(\vec{r}')] x(\vec{r}') G(\vec{r}, \vec{r}') dV' \quad (3)$$

Consider a uniform cylindrical object with a variable dielectric permittivity $\varepsilon(x, y)$, the discrete counterpart of (3) can be obtained as

$$E^v_{scatt(2BA)} = \sum_{l=1}^{N} G^v_{m,l} \tau_l . [E^v_{inc,l} + \sum_{n=1}^{N} G^v_{l,n} \tau_n . E^v_{inc,l}] \quad (4)$$

$$G^v_{m,l} = \frac{-jk_0^2}{4} \int_{Sl} H_0^{(2)}(k_0 \rho(x^v_m, y^v_m, x', y')) dx' dy' \quad (5)$$
$$(m = 1, \cdots, M; l = 1, \cdots, N; v = 1, \cdots, V)$$

where, $v(V)$ is the incident angle, $m(M)$ is the number of measurement points, τ_p is the unknown quantity of the p^{th} sub-domain given by τ=[$\varepsilon(x, y)/\varepsilon_0$-1] and is taken as constant in an element, k_0 is the wavenumber in the external medium, ρ is given by $\rho(x^v_m, y^v_m, x', y') = \sqrt{(x^v_m - x')^2 + (y^v_m - y')^2}$, $H^{(2)}_0(k_0\rho)$ is the zeroth order Hankel functions of the second kind, N is the element number of the mesh.

Under such assumptions, the inverse scattering problem can be recast into a discretized form as

$$\Im = \sum_{v=1}^{V}\sum_{m=1}^{M}\left|E^v_{scat,m} - \sum_{l=1}^{N} G^v_{m,l}\tau_l.[E^v_{inc,l} + \sum_{n=1}^{N} G^v_{l,n}\tau_n.E^v_{inc,l}]\right|^2 \quad (6)$$

$$E^v_{inc}(x,y) = \exp\{j[x\cos\upsilon^v_{inc} + y\sin\upsilon^v_{inc}]\}, v=1,...,V \quad (7)$$

where the incident angle υ^v_{inc} is given by

$$\upsilon^v_{inc} = (v-1)\frac{2\pi}{V}\,(v=1,...,V) \quad (8)$$

The polar coordinates of the m^{th} measurement point are (r, υ^v_m), and r is set to a fixed value and υ^v_m is given by

$$\begin{aligned}&\upsilon^v_m = \partial + \upsilon^v_{inc} + 2(m-1)(\pi - \partial)/(M-1)\\ &m = 1,...,M; \upsilon = 1,...,V\end{aligned} \quad (9)$$

where ∂ is a fixed angle.

To reduce the computational burden of the proposed methodology, one will always test if the condition $\tau \geq \tau_{\min}$ ($\tau_{\min}$ is small constant predefined by the user) is satisfied at the beginning of each iteration step. The computation producer for the term $G\cdot\tau\cdot E$ will be activated only when this condition is satisfied. Such approach is particularly computational efficient when the scatterers are taking up only a few fraction of the whole solution domain.

III. Numerical Validations

The first application is a single weak scatter. The scatter is a homogeneous cylinder of radius $r = 0.4\,\lambda_0$ with τ =1.2. The center of the circular is at (x_0,y_0)=(-0.137 λ_0,-0.137 λ_0). The solution domain of an $a \times a$ (a=λ_0) square is partitioned into N=20 $\times$ 20 sub-domains. 32 observing points are distributed uniformly on a circumference of radius $b = 0.84\,\lambda_0$, and V is set to be 1. Fig. 2 compares the model and the inversed scatting electric fields using the 2BA (2BA) based procedure and the proposed (Proposed) procedure after 50 iterations. The inversed τ is 1.1382 using the 2BA, which is compared to a value of τ=1.22 using the Proposed. Comparisons of the reversed scatting electric fields at the measurement or observation points using the two techniques are given in Fig. 3. Obviously, the Proposed outperforms 2BA in both efficiency and accuracy.

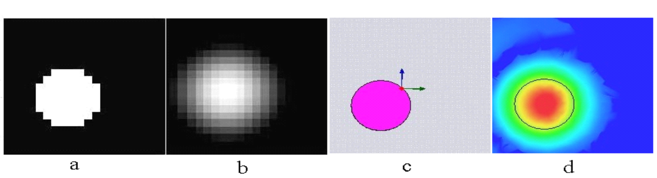

Fig. 2. The original models (a,c) and the reversed scatting electric fields (b,d) using the 2BA based (a,b) and the Proposed (c,d) procedures.

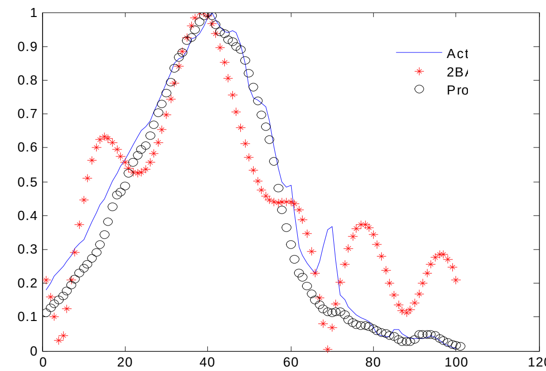

Fig. 3. The actual and the reversed scattering electric fields at the measured points using the 2BA based and the Proposed procedures.

The second application is a multiple strong scatter case. Four homogeneous strong cylindrical scatters of radius r=0.1 λ_0 are centered, respectively, at (-0.11 λ_0, -0.11 λ_0), (0.11 λ_0, -0.11 λ_0), (0.11 λ_0, 0.11 λ_0), (-0.11 λ_0, 0.11 λ_0) with dielectric permittivities of ε_1=3.5 , ε_2=2.0 , ε_3=3.0 , and ε_4=2.0. 100 observing points are distributed uniformly on a circumference of radius b=0.84 λ_0, and V=1. Also, the Proposed and 2BA are employed to inverse the scatters. It is found that it is difficult to obtain accurate results of the scatter parameters using 2BA while sufficiently accurate results of ε_1=3.48 , ε_2=2.14 , ε_3=2.79 , ε_4=1.98 are attained by the Proposed after only 50 iterations. The reversed scattered electric fields on the observing points using the two procedures are compared in Fig. 4. Clearly, the Proposed will reverse a complex nonlinear inverse scattering problem with good accuracies. However, the reliable results of the same problem cannot be realized using available 2BA.

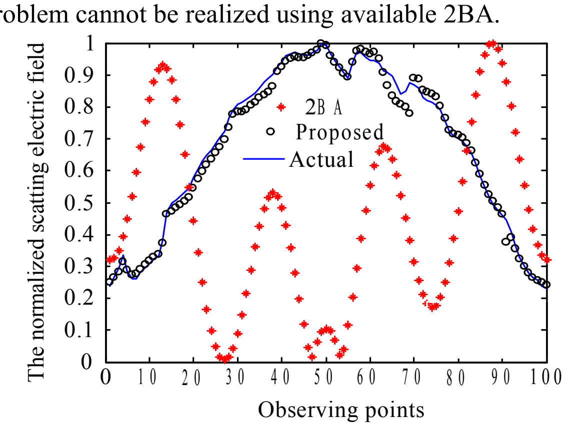

Fig. 4. Comparison of reversed scattered electric fields using different procedures.

IV. References

[1] Salvatore Caorsi, Microwave imaging within the second-order Born approximation: stochastic optimization by a genetic algorithm, *IEEE Trans. AP,* vol.49, pp. 22-31, 2001.

[2] Nikolaus Hansen, Andreas Ostermeier, Completely Derandomized Self-Adaptation in Evolution Strategies, Evolutionary Computation, vol.9, Issue 2, pp. 159-195, 2001.

[3] Shiu Yin Yuen, Chi Kin Chow, A Genetic Algorithm That Adaptively Mutates and Never Revisits, *IEEE Transactions On Evolutionary Computation ,* vol.13, NO. APRIL 2009.